TG–1007
AUGUST 1968
Copy No. 2

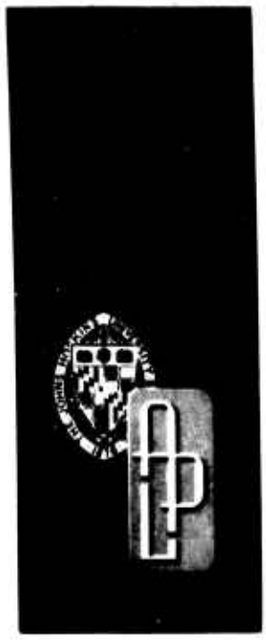

Technical Memorandum

APPROXIMATE FUNCTIONS AS PARTICULAR SOLUTIONS IN THERMAL-STRESS ANALYSIS OF AN OGIVAL RADOME

by MANFORD B. TATE

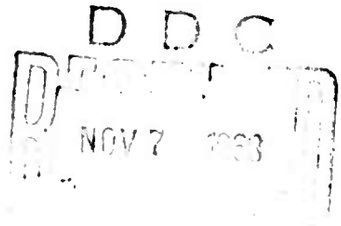

THE JOHNS HOPKINS UNIVERSITY • APPLIED PHYSICS LABORATORY

TG—1007
AUGUST 1968

Technical Memorandum

APPROXIMATE FUNCTIONS AS PARTICULAR SOLUTIONS IN THERMAL-STRESS ANALYSIS OF AN OGIVAL RADOME

by MANFORD B. TATE

THE JOHNS HOPKINS UNIVERSITY ▪ APPLIED PHYSICS LABORATORY
8621 Georgia Avenue, Silver Spring, Maryland 20910

Operating under Contract NOw 62-0604-c, Bureau of Naval Weapons, Department of the Navy

THE JOHNS HOPKINS UNIVERSITY
APPLIED PHYSICS LABORATORY
SILVER SPRING, MARYLAND

ABSTRACT

Functions of approximation to particular solutions that occur in the ogival radome thermal-stress problem are presented. It was found by numerical comparisons with the generating differential equations that the approximate closed-form solutions display an error range of no more than plus or minus one-half percent.

The solutions were derived to gain two major advantages: first, a reduction of analytical complexity lessens the chance of computational error; and, second, certain unwieldiness in numerical work is reduced or eliminated.

Computer results are tabulated for repeated future application in the evaluation of thermal stresses in blunt and pointed radomes of compound-ogive configuration.

THE JOHNS HOPKINS UNIVERSITY
APPLIED PHYSICS LABORATORY
SILVER SPRING MARYLAND

TABLE OF CONTENTS

LIST OF FIGURES

THE JOHNS HOPKINS UNIVERSITY
APPLIED PHYSICS LABORATORY
SILVER SPRING, MARYLAND

I. INTRODUCTION

General analyses of shell stresses are developed in textbooks, References (1) to (5), inclusive, and Boley and Weiner (4) discussed thermal stresses. For heat-variant material properties in the wall of an ogival radome, axisymmetric thermal stresses were studied in Reference (6).

In References (7) and (8), Rivello took up the problem of thermal stress in cylindrical sandwich shells, and Dailey (9) employed the stiffness-matrix method for axisymmetric shells of revolution. Weckesser, Hallendorff and Suess (10) investigated materials for radome construction in high-temperature applications. Thick-walled conical shells were examined by Weiss in Reference (11).

Pyroceram 9606 test data, temperatures around the nose of a blunt radome, the Von Karman shape, temperature distributions in a test radome, and compound-ogive profiles were investigated in References (12) to (16), inclusive, in association with the present subject.

From numerical studies, it was found that particular solutions based on applied temperature distributions obtained as infinite series made computerization more complex, inhibited analytical continuity, and increased an amount of computation that was already rather cumbersome. To offset these difficulties, closed-form approximate solutions applicable to particular cases are developed in the present text. Moreover, computerized data on these solutions are tabulated for future reference.

The ogival radome wall profile is sketched on Figure 1, where dimensions and coordinate variables are defined also. A differential element of the wall is drawn in Figure 2. On it are shown normal-stress resultants (N_ψ, N_θ), bending moments (M_ψ, M_θ), and the shearing-stress resultant (Q_ψ).

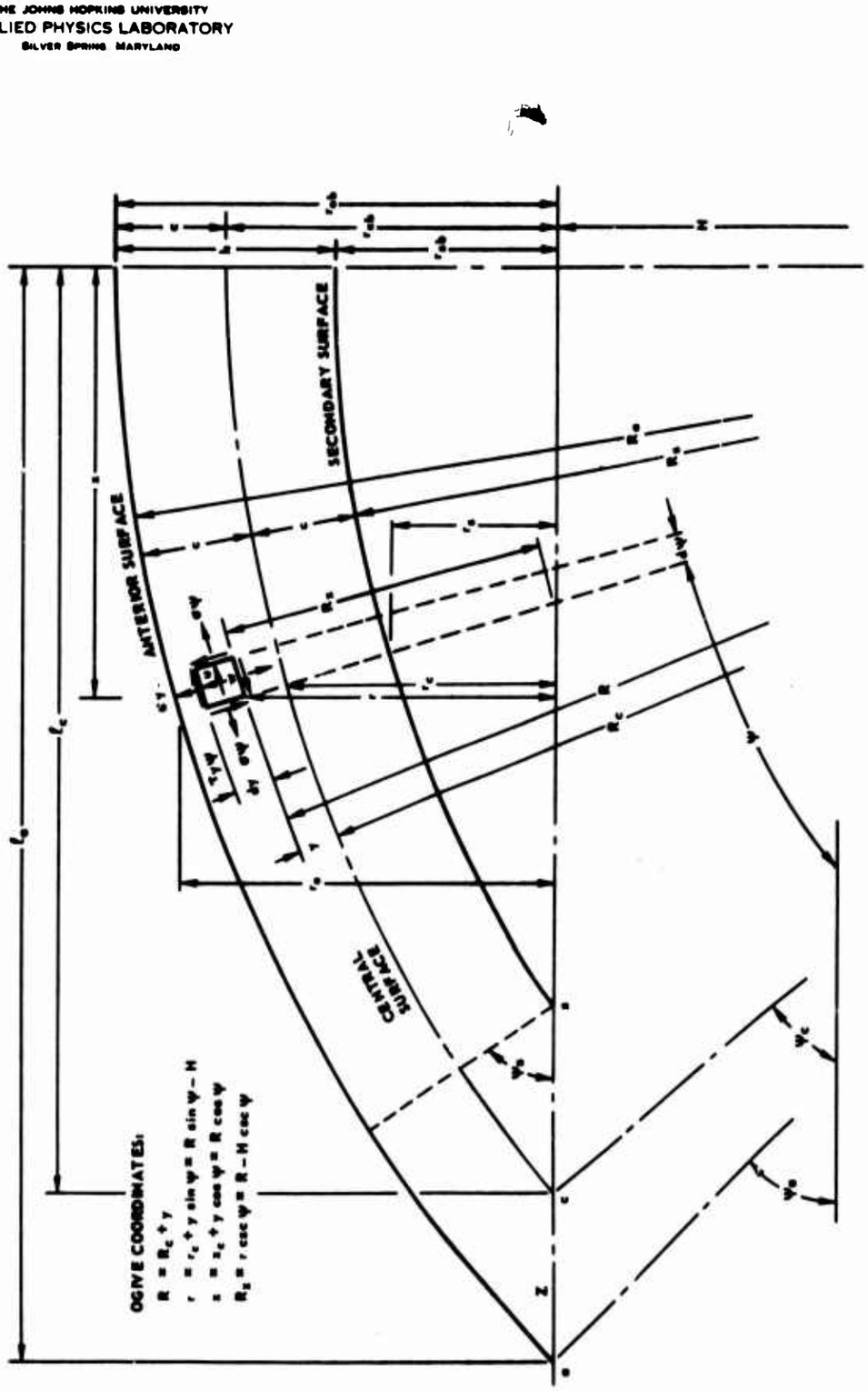

Fig. 1 OGIVAL RADOME WALL DIMENSIONS

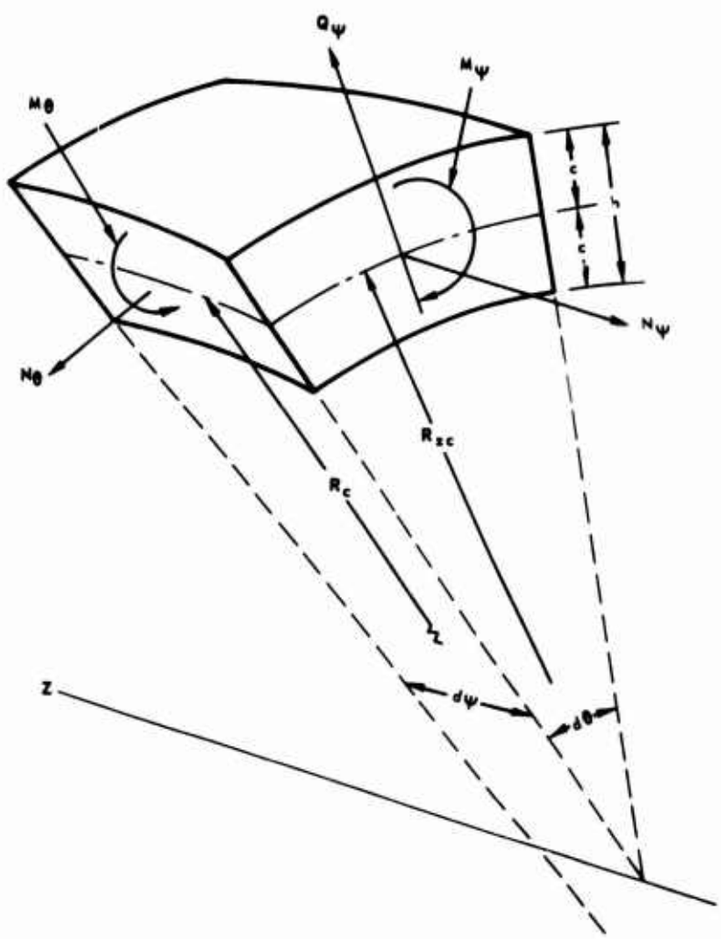

Fig. 2 RADOME-WALL ELEMENT WITH STRESS RESULTANTS AND BENDING MOMENTS

II. ACKNOWLEDGEMENT

The computer work for data in Tables 1 and 2 was programmed by Mr. R. L. McCutcheon of the APL/JHU Computer Center.

III. NOMENCLATURE

A,B:	Constants
E:	Young's modulus of elasticity, psi
J,K:	Constants
L:	Operator
M:	Bending-moment resultant, ippi
N:	Normal-stress resultant, ppi
Q:	Shearing-stress resultant, ppi
R:	Radius, inches
V:	Wall-slope function, radians per inch
Z:	Geometric axis of radome
c:	Radome-wall half thickness (c = h/2), inches
h:	Radome-wall thickness, inches
ℓ:	Span length of radome, inches
q:	Auxiliary shear function, ppi
r:	Radius, inches
Δ:	Denominator
β:	Wall-bending parameter, radians
θ:	Coordinate angle of rotation, degrees or radians
ν:	Poisson's ratio
χ:	Radome-wall curvature change, radians per inch
ψ:	Coordinate angle of azimuth, degrees or radians

The following notations are employed as subscripts:

a:	Anterior or outer surface of radome
b:	Base of radome
c:	Central surface of radome wall
g:	General
i,j:	Numerical indices: 0, 1, 2, 3,...
o:	Origin or initial value (zero)
p:	Particular
s:	Secondary or inner surface of radome
v:	Pertaining to wall slope (V)
R,θ,ψ:	Spherical-coordinate directions

IV. REFERENCE EQUATIONS

The differential equations derived in Reference (6) are:

$$(L^2+\nu)(q+K_3) = EhV + (1-\nu)K_1 \frac{r_c}{R_c} + \frac{K_2 R_c}{r_c \tan\psi} \tag{1}$$

$$(L^2-\nu)(EhV) = (\nu^2+\beta^4)\left[\frac{J_1 r_c}{R_c^2} + \frac{J_3}{R_c} - q\right] \tag{2}$$

In these expressions, q is the auxiliary shear function defined by equation (3) wherein Q_ψ is resultant or total shear, V represents change in slope of the radome wall, ν is Poisson's ratio, E is Young's modulus of elasticity, L is the operator defined below in equation (4), r_c and R_c are the radii pictured in Figure 1 where the coordinate angle ψ also is shown, and the other terms are constants.

$$q = \frac{r_c Q_\psi}{R_c \sin\psi} \tag{3}$$

$$L^2 q = \frac{r_c}{R_c \sin\psi}\frac{d^2q}{d\psi^2} + \cot\psi \frac{dq}{d\psi} - \frac{qR_c \cos\psi}{r_c \tan\psi} \tag{4}$$

Solutions of differential equations (1) and (2) are obtained as

$$q = q_p + q_g, \qquad V = V_p + V_g \tag{5}$$

where subscripts p, g denote the particular and general solutions, respectively. Our purpose herein is to develop functions of approximation to the particular solutions.

V. TOTAL SHEAR

The total shear (Q_ψ) can be calculated with equation (3) from function q for which the particular solution q_p is given approximately by

$$q_p = B_5 + \frac{r_c B_8}{R_c} + \frac{R_c(B_7 + B_8 \cos\psi)}{r_c \tan\psi} \tag{6}$$

wherein the B_i are constants, and the remaining quantities are illustrated in Figures 1 and 2.

VI. WALL-SLOPE CHANGE

The particular part V_p of slope change V of the radome-wall profile is calculated approximately with

$$V_p = B_8' - \frac{r_c B_8'}{R_c} - \frac{R_c (B_7' + B_8' \cos\psi)}{r_c \tan\psi} \tag{7}$$

where the B_i' are constants, and the radii (r_c, R_c) and the coordinate angle are identified in Figure 1.

VII. NORMAL-STRESS RESULTANTS

The normal-stress resultants are expressed in terms of the foregoing relations as follows:

$$N_{\psi p} = \frac{q_p R_c \cos\psi}{r_c} \tag{8}$$

$$N_{\theta p} = \left[B_8 - \frac{B_8 R_c}{r_c}\right] \cos\psi - \frac{R_c}{r_c} \left[\csc^2\psi + \frac{R_c \cos\psi}{r_c \tan\psi}\right] (B_7 + B_8 \cos\psi) \tag{9}$$

which contain the constants and variables referred to in connection with equation (6).

VIII. BENDING CURVATURES

The components of curvature change produced by bending of the radome wall are:

$$\chi_{\theta p} = \frac{V_p \cos\psi}{r_c} \tag{10}$$

$$\chi_{\psi p} = \left[\frac{B_8'}{r_c} - \frac{B_8'}{R_c}\right] \cos\psi + \frac{1}{r_c} \left[\csc^2\psi + \frac{R_c \cos\psi}{r_c \tan\psi}\right] (B_7' + B_8' \cos\psi) \tag{11}$$

which contain the constants and variables referred to in connection with equation (7).

IX. TEMPERATURE FUNCTIONS

As developed in Reference (6), temperature functions are defined by the following expressions.

$$\sigma_t = E\epsilon_t/(1-\nu) \tag{12}$$

$$N_{t\psi} = \int_{-c}^{+c} \frac{r\sigma_t dy}{r_c}, \qquad N_{t\theta} = \int_{-c}^{+c} \frac{R\sigma_t dy}{R_c} \tag{13}$$

$$M_{t\psi} = \int_{-c}^{+c} \frac{r\sigma_t y dy}{r_c}, \qquad M_{t\theta} = \int_{-c}^{+c} \frac{R\sigma_t y dy}{R_c} \tag{14}$$

With $x = y/c$, the thermal strain (ϵ_t) obtained in Reference (12) can be written as follows.

$$\epsilon_t = (-241.2 + 3.445T) \times 10^{-6}, \quad -1 \le x \le 0 \tag{15}$$

$$= (-119.1 + 2.958T) \times 10^{-6}, \quad 0 \le x \le 0.5 \tag{16}$$

$$= (+190.3 + 2.221T) \times 10^{-6}, \quad 0.5 \le x \le 1 \tag{17}$$

The preceding relations are applicable to the entire radome for the temperature range of

$$70°F \le T \le 1400°F \tag{18}$$

and are used together with T, which is expressed by

$$T = T(x,\psi) = f(x)\ T_a(\psi) \tag{19}$$

where T_a is the outer-surface temperature distribution plotted on Figure 3. The spanwise linear temperature distribution shown in Figure 3 as

$$T_a = T_a(\psi) = 589 + 705 \cos\psi \tag{20}$$

was employed in the reported computations. And f(x) giving the distributive character over the thickness of the wall is

$$f(x) = \sum_{n=0}^{3} f_n x^n = 0.257 + 0.358x + 0.305x^2 + 0.084x^3 \tag{21}$$

wherein the polynomial coefficients f_n are shown in the expanded form on the right.

When the integrations of equations (13) and (14) are carried out with equations (12) and (15) to (21), the resultant temperature functions are obtained as written below.

$$N_{t\theta} = K_o + K_1 \cos\psi, \qquad N_{t\psi} = N_{t\theta} + \frac{R_c}{r_c}(K_2 + K_3 \cos\psi) \tag{22}$$

$$M_{t\theta} = J_o + J_1 \cos\psi, \qquad M_{t\psi} = M_{t\theta} + \frac{R_c}{r_c}(J_2 + J_3 \cos\psi) \tag{23}$$

The constants J_i, K_i are the same as those appearing in equations (1) and (2) and, by the methods just described, were found to be

$$K_o = 4.648Eh/(1-\nu) \times 10^4, \quad K_1 = 6.792Eh/(1-\nu) \times 10^4 \tag{24}$$

$$K_2 = 4.393Eh/(1-\nu) \times 10^7, \quad K_3 = 3.420Eh/(1-\nu) \times 10^7 \tag{25}$$

$$J_o = 1.269Eh^2/(1-\nu) \times 10^4, \quad J_1 = 0.989Eh^2/(1-\nu) \times 10^4 \tag{26}$$

$$J_2 = 1.704Eh^2/(1-\nu) \times 10^7, \quad J_3 = 2.195Eh^2/(1-\nu) \times 10^7 \tag{27}$$

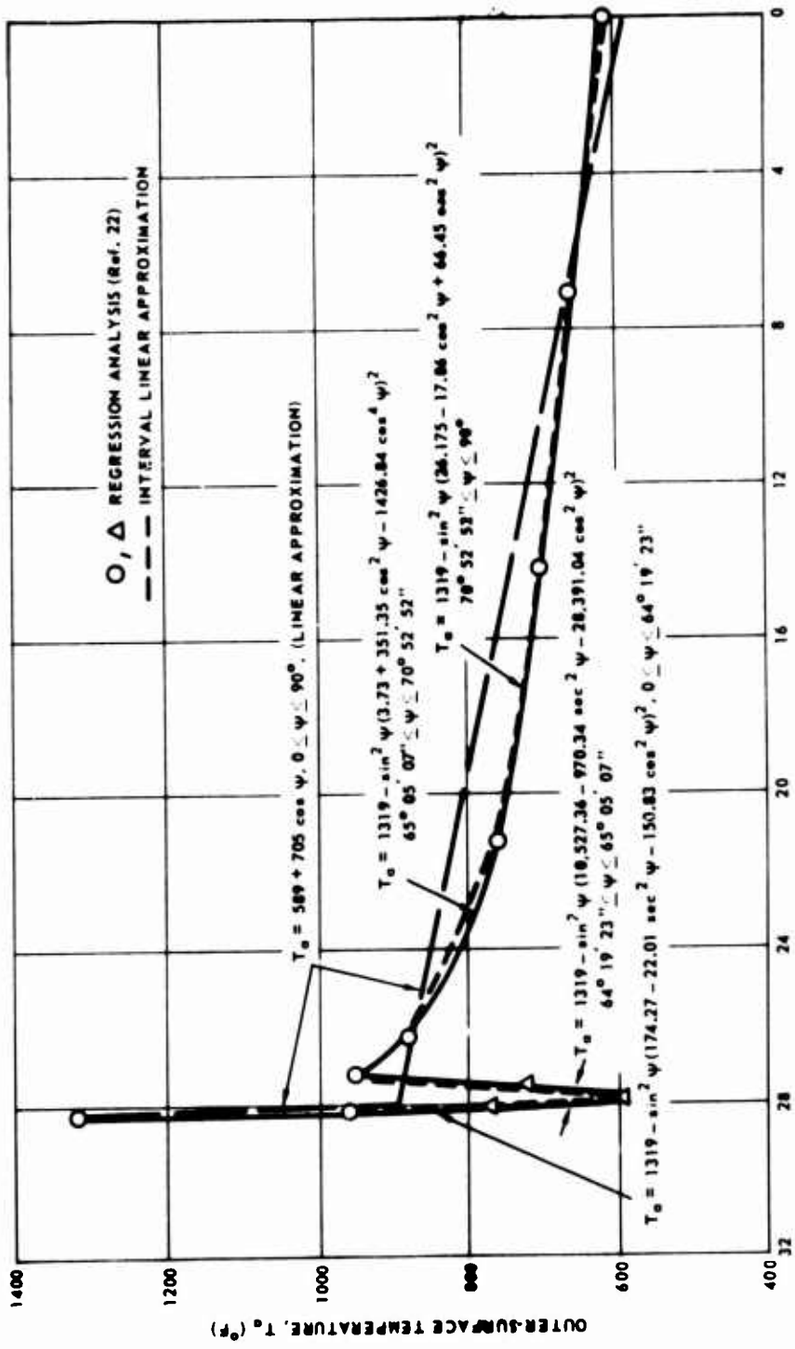

Fig. 3 SPANWISE TEMPERATURE DISTRIBUTION FOR BICENTRIC-OGIVE RADOME

and the material properties were evaluated from test data on Pyroceram 9606 in Reference (12); i.e.,

$$E = 16{,}400{,}000 \text{ psi} \qquad \nu = 0.244 \tag{28}$$

where E is accurate within four percent and ν within 2.5 percent over temperature range (18).

X. DETERMINATION OF CONSTANTS

By putting expressions (6) and (7) into (1) and (2), we secure formulas for numerical determination of constants B_i and B_i'. These constants are computed in the following sequence.

$$B_8 = \frac{J_1}{R_c} - \frac{(1-\nu^2)(J_1 + K_1 R_c)}{(1+\beta^4) R_c}, \qquad B_8' = \frac{(1-\nu)(\nu^2+\beta^4)(J_1 + K_1 R_c)}{(1+\beta^4) Eh R_c} \tag{29}$$

$$A_8 = \frac{(\nu^2+\beta^4)(J_3 + K_3 R_c)}{R_c \Delta_8}, \qquad B_8 = A_8 - K_3 \tag{30}$$

$$\Delta_8 = \beta^4 - 2 + \frac{2\Delta_3^2}{\beta^4 - 2 + \Delta_3^2}, \qquad \beta^4 = -\nu^2 + 12(1-\nu^2)(R_c/h)^2 \tag{31}$$

$$\Delta_3 = \left[(3 + \cot^2\psi) + \frac{r_c(3 + 2\cot^2\psi)}{R_c \sin\psi} \right]_{\text{mean}} \tag{32}$$

$$\beta_8 = \frac{A_8 + \Delta_3}{\beta^4 - 2 + \Delta_3^2}, \qquad B_8' = \frac{A_8 - (\Delta_3 + \nu)B_8}{Eh} \tag{33}$$

$$B_8' = \frac{\nu A_8 + 2B_8}{Eh} \tag{34}$$

$$B_7 = \frac{(\Delta_2 - \nu)K_2}{\Delta_2^2 + \beta^4}, \qquad B_7' = \frac{(\nu^2 + \beta^4)K_2}{(\Delta_2^2 + \beta^4)Eh} \tag{35}$$

$$\Delta_2 = 2\left[1 + \frac{r_c}{R_c \sin^3\psi} \right]_{\text{mean}} \tag{36}$$

For slender ogives, $\cot\psi$ and r_c/R_c are small and $\sin\psi$ approaches unity. The terms (32) and (36), therefore, have slight variation, and one can employ mean values computed as arithmetical averages with initial and final values of the coordinates. For the bicentric-ogive radome described in Reference (16), we have

$$r_{c1} = 0.238", \qquad \psi_1 = 64^\circ\ 19'\ 23" \tag{37}$$

$$r_{cb} = 6.625", \qquad \psi_b = 90^\circ \tag{38}$$

$$\quad = 0.25", \qquad R_c = 64.679" \tag{39}$$

and the numerical results are listed in Tables 1 and 2.

XI. COMPUTER RESULTS

As part of the overall computer program, values of the functions occurring in the particular solutions were calculated in Program Problem 164. The associated constants are reported in Table 1; and functional numerical data, in Table 2. All of the computer results that are reported in Tables 1 and 2 were computed and stored in double precision but shown here in single precision. The double precision numbers are needed in simultaneous solutions for general constants of integration, which are evaluated from specified boundary conditions imposed at the juncture between nosecap and mainbody and at the base of the radome where it is joined to a missile body.

XII. DISCUSSION

Formulation of closed-form approximate particular functions (q_p, V_p, $N_{\theta p}$, $\chi_{\psi p}$) are presented as equations (6), (7), (9), and (11) for the mainbody of the bicentric-ogive radome described in Reference (16). They were programmed for numerical evaluation at thirteen points along the length of the mainbody lying in the interval $\psi_1 \leq \psi \leq 90^\circ$, where $\psi_1 = 64^\circ\ 19'\ 23"$ and the base of the radome is located at 90° (Figure 1).

The results are reported for future reference, because they are used in each analysis of thermal stress and deformation irrespective of the boundary conditions imposed on the radome. Specific values occur in the fulfillment of boundary requirements which provide simultaneous equations that occur in calculation of integration constants appearing in the general integrals of differential equations (1) and (2).

One can observe from Table 2 that q_p increases monotonically from the nosecap junction (at ψ_1) to the radome base (at 90°). But total shear in the particular solution behaves oppositely as computed with the following relation.

Table 1. Constants in Closed-Form Particular Solutions

Symbol	Value	Symbol	Value
β^4	755,387.78	B_6	$0.460,533 \times 10^{-2}$
Δ_2	2.24	B_8	2.067,534
Δ_3	3.25	B_7	$0.629,548 \times 10^{-5}$
Δ_5	755,385.79	B_8	$0.799,994 \times 10^{-5}$
$\beta^4 + \Delta_2^2$	755,392.81	B_6'	$0.110,662 \times 10^{-6}$
$\beta^4 - 2 + \Delta_3^2$	755,396.35	B_8'	6.795,812
		B_7'	$0.581,105 \times 10^{-6}$
A_5	1.859,424	B_8'	$0.453,511 \times 10^{-6}$

Table 2. Functional Values of Particular Solutions

j	Ψ (d-m-s)	$\frac{q_p \times 10^3}{Eh}$	$\frac{N_{\theta p} \times 10^3}{Eh}$	$V_p \times 10^4$	$R_c \chi_{\Psi p} \times 10^4$
1	64-19-23	0.328,962,85	18.083,065	-1.040,084,8	119,874,77
2	65-06-39	0.605,553,02	20.680.353	-0.438,696,15	14,835,188
3	66-45-43	1.191,282,1	19.793,691	- .296,856,92	0.662,232,44
4	68-31-56	1.781,837,4	18.415,570	- .312,404,94	- 1.191,796,8
5	70-27-15	2.373,419,8	16,851,096	- .361,440,69	- 1.621,952,3
6	72-01-27	2.817,373,3	15,549,685	- .406,894,98	- 1.671,379,0
7	73-44-23	3.261,446,1	14.110,889	- .456,230,82	- 1.611,040,9
8	75-27-58	3.664,639,9	12.648,412	- .503,095,07	- 1.492,807,3
9	77-25-18	4.067,873,5	10.976,944	- .551,223,87	- 1.322,628,6
10	79-06-45	4.370,315,4	9.521,078,6	- .587,846,96	- 1.157,576,3
11	81-06-53	4.672,765,4	7.785,791,5	- .624,688,70	- 0.948,900,12
12	83-43-13	4.975,213,2	5.513,499,7	- .661,404,10	- .663,819,83
13	90°	5.277,579,8	- 0.001,[illegible]9,1	- .694,981,63	+ .056,732,43

$$Q_{\psi p} = \frac{q_p R_c \sin\psi}{r_c} \tag{40}$$

Here, the sine increases from $\sin\psi_1 = 0.901250$ to $\sin\psi_b = 1$; and r_c/R_c, from 0.003679 to 0.102429. Therefore

$$Q_{\psi p}(\psi_1) = 80.586{,}510\text{Eh} \times 10^{-8} = 3.304 \text{ ppi} \tag{41}$$

$$Q_{\psi p}(90°) = 51.524{,}273\text{Eh} \times 10^{-8} = 2.112 \text{ ppi} \tag{42}$$

and similar comparisons can be made for the other functions in Table 2.

XIII. CONCLUDING REMARKS

Approximate functions for particular solutions of governing differential equations are presented in the text. They were developed to avoid cumbersome infinite series and to express the relevant functions in closed form. The generating equations are satisfied (numerically) by the derived expressions such that discrepancies lie in a range of plus or minus one-half percent.

Major advantages of these solutions are simplification that reduces the likelihood of numerical errors and certain unwieldy characteristics in numerical work are minimized or eliminated.

Computerized data on ogival radome thermal-stress functions are collected that can be used in future stress calculations.

REFERENCES

(1) A. E. H. Love, "The Mathematical Theory of Elasticity," 4th ed, Cambridge University Press, Cambridge, England, 1927; 1st American printing, Dover Publications, New York, 1944.

(2) S. Timoshenko and J. N. Goodier, "Theory of Elasticity," 2d ed, McGraw-Hill, New York, 1951.

(3) S. Timoshenko and S. Woinowsky-Krieger, "Theory of Plates and Shells," McGraw-Hill, New York, 1959.

(4) B. A. Boley and J. H. Weiner, "Theory of Thermal Stresses," Wiley, New York, 1960.

(5) W. Flugge, "Stresses in Shells," Springer, Berlin, 1960.

(6) M. B. Tate, "Axisymmetric Thermal Stresses in Ogival Radome Walls Having Material Properties that Change with Heat Intensity," APL/JHU BBE EM-3976, 1965.

(7) R. M. Rivello, "Thermal Stress Analysis of Sandwich Cylinders," APL/JHU TG-721, 1965.

(8) _____ "Thermal Stresses in Finite Length Sandwich Cylinders," APL/JHU TG-903, 1967.

(9) G. Dailey, "Numerical Solutions of Axisymmetric Thermal Stress Problems," APL/JHU TG-876, 1966.

(10) L. B. Weckesser, R. H. Hallenborff, and R. P. Suess, "Environmental Limitations of Alumina, Fused Silica and Pyroceram 9606 Radomes," (Confidential), APL/JHU TG-865, 1967.

(11) R. O. Weiss, "The Thermal Stresses in a Thick-Walled Cone by the Method of Finite Differences," APL/JHU TG-914, 1967.

(12) M. B. Tate, "Functionalization of Pyroceram 9606 Test Data for Radome Thermal-Stress Analysis," APL/JHU TG-980, 1968.

(13) _____, "Air Properties and Flow Conditions Around the Nose of a Blunt Radome," APL/JHU TG-981, 1968.

(14) _____, "Curvature Radii and Derivatives for Thermal-Stress Analysis of Von Karman Radomes," APL/JHU TG-982, 1968.

(15) _____, "Statistical Analysis of Temperature Data from Wind Tunnel Test of a Von Karman Radome," APL/JHU TG-983, 1968.

(16) _____, "Compound-Ogive Radomes as Substitute Structures for Von Karman Shapes," APL/JHU TG-985, 1968.

UNCLASSIFIED
Security Classification

DOCUMENT CONTROL DATA - R & D

(Security classification of title, body of abstract and indexing annotation must be entered when the overall report is classified)

1. ORIGINATING ACTIVITY (Corporate author)	2a. REPORT SECURITY CLASSIFICATION
The Johns Hopkins Univ., Applied Physics Lab. 8621 Georgia Ave. Silver Spring, Md. 20910	Unclassified
	2b. GROUP N. A.

3. REPORT TITLE

Approximate Functions as Particular Solutions in Thermal-Stress Analysis of an Ogival Radome

4. DESCRIPTIVE NOTES (Type of report and inclusive dates)

Technical Memorandum

5. AUTHOR(S) (First name, middle initial, last name)

Manford B. Tate

6. REPORT DATE	7a. TOTAL NO. OF PAGES	7b. NO. OF REFS
August 1968	15	16

8a. CONTRACT OR GRANT NO.	9a. ORIGINATOR'S REPORT NUMBER(S)
NOw 62-0604-c b. PROJECT NO.	TG-1007
c. d.	9b. OTHER REPORT NO(S) (Any other numbers that may be assigned this report)

10. DISTRIBUTION STATEMENT

This document has been approved for public release and sale; its distribution is unlimited.

11. SUPPLEMENTARY NOTES	12. SPONSORING MILITARY ACTIVITY
	NAVORDSYSCOM ORD-03511, Zip 20390

13. ABSTRACT

Functions of approximation to particular solutions that occur in the ogival radome thermal-stress problem are presented. It was found by numerical comparisons with the generating differential equations that the approximate closed-form solutions display an error range of no more than plus or minus one-half percent.

The solutions were derived to gain two major advantages: first, a reduction of analytical complexity lessens the chance of computational error and, second, certain unwieldiness in numerical work is reduced or eliminated.

Computer results for repeated future application in the evaluation of thermal stresses in blunt and pointed radomes of compound-ogive configuration are tabulated.

DD FORM 1 NOV 65 1473

UNCLASSIFIED
Security Classification

14. KEY WORDS

Thermal stress
Ogival radome thermal-stress analysis
Approximate functions for thermal stress
Particular solutions for ogival radome